APPENDIX AVAILABLE ON THE HEI WEBSITE

Research Report 199

Real-World Vehicle Emissions Characterization for the Shing Mun Tunnel in Hong Kong and Fort McHenry Tunnel in the United States

Xiaoliang Wang et al.

Appendix B. Quality Control and Quality Assurance of Field and Laboratory Data

This Appendix was reviewed solely for spelling, grammar, and cross-references to the main text. It has not been formatted or fully edited by HEI. This document was reviewed by the HEI Review Committee.

Correspondence may be addressed to Dr. Xiaoliang Wang, Desert Research Institute, 2215 Raggio Pkwy., Reno, NV 89512; e-mail: *xiaoliang.wang@dri.edu*.

Although this document was produced with partial funding by the United States Environmental Protection Agency under Assistance Award CR–83467701 to the Health Effects Institute, it has not been subjected to the Agency's peer and administrative review and therefore may not necessarily reflect the views of the Agency, and no official endorsement by it should be inferred. The contents of this document also have not been reviewed by private party institutions, including those that support the Health Effects Institute; therefore, it may not reflect the views or policies of these parties, and no endorsement by them should be inferred.

© 2019 Health Effects Institute, 75 Federal Street, Suite 1400, Boston, MA 02110-1817

APPENDIX B. QUALITY CONTROL AND QUALITY ASSURANCE OF FIELD AND LABORATORY DATA

Standard Operating Procedures

Field sampling in the tunnels followed Standard Operating Procedures (SOPs). The SOPs describe monitoring or sampling requirements, acceptance testing procedures, preparation, installation, sample collection, handling and preservation, data acquisition, routine maintenance, routine service checks, calibrations, QC checks, and audit procedures. When a SOP was not available, the manufacturers' operation manuals were followed to operate and service the instruments. Table B.1 lists the field measurement SOPs applicable to the tunnel study.

Sample preparation, shipping/receiving, setup, and recovery procedures for integrated measurements and activities are described in the SOPs given in Table B.2. Filter packs, DNPH cartridges, and XAD-4 cartridges for the integrated sampling channels were prepared in clean laboratories and shipped to and from the field in cooled (<4°C) containers containing max/min temperature recorders. Filter and DNPH samples were stored in refrigerators while XAD-4 samples were stored in freezers before and after sampling. Shipments were coordinated between the field and laboratory by means of a semi-automated chain-of-custody system. Sample identifiers were bar-coded to indicate sample type, analysis type, and sampling time and location. These identifiers were entered into field and laboratory data acquisition systems to track sample status at any time during the study.

Table B.1. Standard Operating Procedures (SOPs) for the Field Measurements

SOP No.	Instrument	SOP Title	Rev. Date
DRI SOP #1-238r1	TSI DustTrak DRX	Standard Operating Procedure for TSI DustTrak DRX Aerosol Monitor Model 8533/8534	08/11/09
DRI SOP #1-211r1	TSI SMPS/CPC	TSI Scanning Mobility Particle Sizer (SMPS): Operation and Maintenance	05/01/06
DRI SOP #1-231r1	DRI medium-volume multichannel sampling system	Standard Operating Procedure for DRI MEDVOL Gas/Particle Sampler for Simultaneous Collection of Gases and $PM_{2.5}$ or PM_{10} on Four Filter Packs	10/01/94
DRI SOP #1-750.4	DRI 1 Channel Fine Particle/SVOC Sampler	Operation of DRI 1-Channel Fine Particle/Semi-Volatile Organic Compound Sampler	7/15/09
DRI SOP #1-710r3	DRI sampler with DNPH cartridge	DRI Carbonyl Sampler	06/12/97
DRI SOP #1-702br3	DRI canister sampler	Operation of DRI 3-Canister Sampler	6/02/97
TBD	ATEC Model 8000 Cartridge Samplers	Standard Operating Procedure for Sampling of oxygenated volatile organic compounds (Hong Kong Chinese University)	2013
DRI SOP 1-250r1	DRI resuspension system	Resuspension of Bulk Samples onto Teflon and Quartz Filters	1/21/05

Laboratory gravimetric and chemical analysis SOPs are summarized in Table B.3. Several common QC activities take place for all analyses: 1) acceptance-testing for contamination of substrates, reagents, extraction vials prior to use; 2) field and laboratory blank designation and analysis to determine blank levels and variability; 3) periodic performance tests of zero and span values for field and laboratory instruments to determine reproducibility and calibration drift; 4) periodic multi-point calibrations in the range of ambient concentrations to determine linearity and concentration relationships; and 5) data validation flags for field and laboratory operations that indicate deviations from procedures. Results from these common quality control activities were recorded in logbooks.

Table B.2. Sample Preparation and Handling Standard Operating Procedures (SOPs)

SOP No.	Observable/Method	Title	Rev. Date
DRI SOP #2-104r3	Filter preparation for gas sampling	Impregnating, Drying, and Acceptance Testing of Filters for Sampling Gases in Air	12/12/94
DRI SOP #2-106r6	Quartz-fiber filter pretreatment	Pre-firing and Acceptance Testing of Quartz Fiber Filters for Aerosol and Carbonaceous Material Sampling	7/30/07
DRI SOP #2-108r4	Sectioning of filters	Sectioning of Teflon and Quartz Filter Samples	4/5/13
DRI SOP #2-110r4	Filter pack processing	Filter Pack Assembling, Disassembling, and Cleaning	11/24/98
DRI SOP #2-117r0	Filter pack shipping and receiving	Filter Pack Sample Shipping, Receiving, and Chain-of-Custody	11/1/12
DRI SOP #1-701r4	Canister preparation	Canister Cleaning and Certification	7/6/98

Table B.3. Laboratory-Related Standard Operating Procedures (SOPs)

SOP No.	Observable/Method	Title	Rev. Date
DRI SOP #2-114r9	PM mass	$PM_{2.5}$ FRM Gravimetric Analysis	10/13/12
DRI SOP #2-203r9	Anions (Cl^-, NO_3^-, and SO_4^{2-})	Anion Analysis of Filter Extracts and Precipitation Samples by Ion Chromatography	10/08/14
DRI SOP #2-208r4	Cations (Na^+, NH_4^+, Mg^{2+}, K^+, and Ca^{2+})	DRI Standard Operating Procedure for Cation Analysis of Filter Extracts and Precipitation Samples by Ion Chromatography	10/08/14
DRI SOP #2-209r8	~51 elements from Na to U	X-ray Fluorescence (XRF) Analysis of Aerosol Filter Samples (PANalytical Epsilon 5)	10/03/14
DRI SOP #2-216r3	OC and EC by IMPROVE method	DRI Model 2001 Thermal/Optical Carbon Analysis (TOR/TOT) of Aerosol Filter Samples – Method IMPROVE_A	10/22/12
DRI SOP #2-219r3	Non-polar organic compounds on filters	In-Injection Port Thermal Desorption and Subsequent Gas Chromatography/Mass Spectrometry Analysis of Non-Polar Organic Species in Aerosol Filter Samples	02/02/10
DRI SOP #2-704.2	Volatile organic compounds (C2-C12)	Analysis of VOC in Ambient Air by Gas Chromatography and Mass Spectrometry	6/22/04
DRI SOP #2-701.2	CO, CO_2 and CH_4	Canister-Based Analysis of CO, CO_2 and CH_4 by Gas Chromatography with Flame Ionization Detection	3/30/05
DRI SOP #2-710r4	Carbonyls (DNPH/HPLC)	Analysis of Carbonyl Compounds by High Pressure Liquid Chromatography	4/11/05
EN-G-101.v3	Carbonyls (DNPH/HPLC)	Determination of Carbonyl Compounds in Ambient Air with DNPH-Silica Cartridges (Hong Kong Premium Services and Research Laboratory)	1/31/14
DRI SOP #2-750.6	SVOCs	Analysis of Semi-Volatile Organic Compounds by Gas Chromatography and Mass Spectrometry	11/28/11
EN-P-102.v1	SVOCs	Determination of Semi-Volatile Organic Compounds (SVOC) in Gaseous and Particle Phases (Hong Kong Premium Services and Research Laboratory)	4/10/14
DRI SOP #3-003r6	EAF field, mass, and chemical data processing and validation	Dry Deposition Field, Mass, and Chemical Data Processing and Validation	7/30/07
DRI SOP #3-201r1	OAL field and chemical data processing and validation	Data Processing and Validation	1/11/05

Sample Collection

All samplers were cleaned, tested, and leak checked prior to deployment. Criteria for passing leak test was <5% of nominal flow measured at inlet under vacuum. Independent digital flow meters were used for pre- and post-sample flow rate measurements in the field. Sample lines were disconnected at the inlet point of each sampler and the flow meter was connected while the flow rate was measured and adjusted, if necessary. Measured flow rates as indicated on the meters were recorded on field data sheets for each sample. The flow meters were calibrated against a reference standard (dry gas meter for flows >20 L/min and electronic bubble meter for flows <20 L/min) before and after each field campaign. Least squares linear regression equations were calculated from the calibration data for each device and used to adjust the recorded flow rates to actual volumetric flow rates at local conditions before calculating sample volumes. The adjustment was done automatically by the data processing software for SVOC samples, by manually adjusting the flow rates input to the database for DNPH, and in post-analysis data processing for filter samples.

For each sample collected, a field data sheet was filled out by the operator that recorded the media ID number, location, start and end times, initial and final flow rates, and any exceptional conditions that occurred during the sample. This information was transcribed into a database table using computer data entry forms designed for each media type. The field data information entered was reviewed for errors and inconsistencies and corrected, as needed, based on comparison with operator notes and information from concurrent samples on other media types. After review, the field data were used to calculate sample volumes and provide identification of analytical results using data processing software. The software also performs field blank subtractions and calculates analytical uncertainties based on replicate sample analyses.

Evaluation of Field Data

The CO, NO_x, and SO_2 analyzers used in the SMT study were audited and calibrated three times during field measurement (all in first month from January 19 to February 16, 2016) and once after field measurement completion by the audit team from the Hong Kong Polytechnic University. The efficiency of NO_2 converters on the NO_x analyzers was checked after the field measurement and found to be 96.95-98.95% at NO concentrations of 100-460 ppbv. No calibration was done during the second month from March 2 through March 31, 2016. Figure B.1 shows the calibration curves of the CO, NO, and SO_2 analyzers. The coefficient of variation (COV) of the ratio between audit and measured concentrations during field measurement was <6% except the inlet SO_2 analyzer, which was 18%. Because only three calibrations were conducted during the SMT study, the slope and intercept of the calibration equations were interpolated or extrapolated and applied to the corresponding raw data. While most gas analyzers showed similar concentrations and diurnal patterns in both months, the CO analyzer at the outlet site showed a baseline drift and the NO_x analyzer showed higher concentrations level after March 1, 2015. Due to the lack of calibration data after March 2, the CO and NO_x data analysis was limited to the period of January 19 to February 16, 2015, and the 40 sampling periods in March were not included in further analysis. Data from eight NO_x sampling periods were treated as outliers and invalidated. The outlet NO_x concentrations on January 21, 2015 were 60-70% of those in neighboring days, while the inlet NO_x concentrations were similar to neighboring days, resulting in the outlet concentrations lower than the inlet concentrations. Traffic video and vehicle counts did not show differences between January 21 and neighboring days. The outlet NO_x concentrations on January 21, 2015 (four sampling periods) was invalidated. The outlet NO_x data on February 10, 2015 (four sampling periods) showed abnormally constant values and was invalidated. The SO_2 data at both inlet and outlet sites did not show drift or concentration change in the first and second months, and therefore both months' data were analyzed and reported.

Figure B.2 plots the CO_2 calibrations before and after the SMT field measurement showing that the COVs were <2% before and after field measurement. Therefore, the regression equations through all calibration points were used to adjust the respective inlet and outlet CO_2 concentrations.

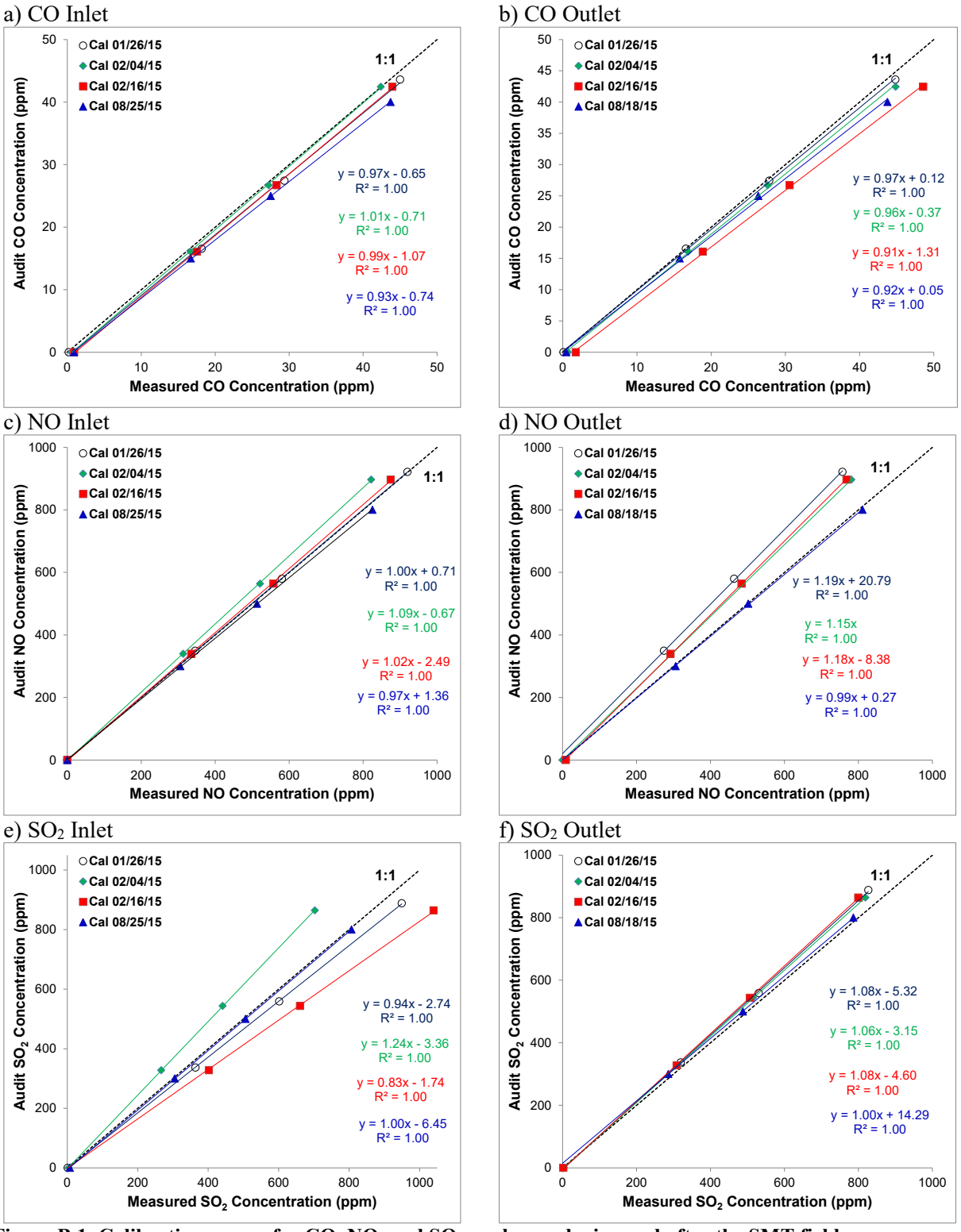

Figure B.1. Calibration curves for CO, NO, and SO_2 analyzers during and after the SMT field measurement in 2015.

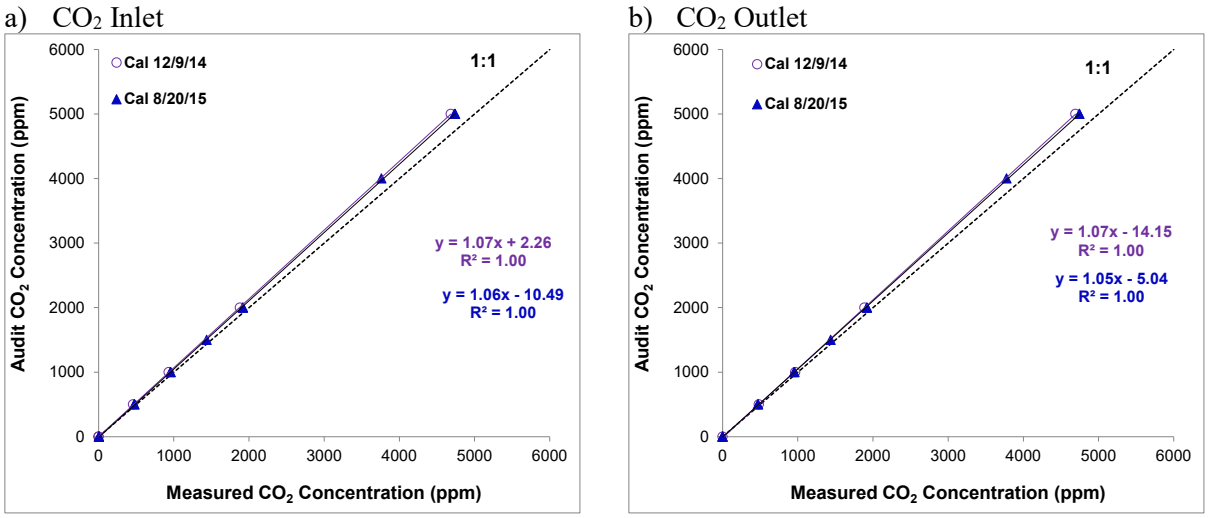

Figure B.2. Calibration curves for CO_2 analyzers before and after the SMT field measurement on 12/9/14 and 8/20/15, respectively.

Figure B.3 compares $PM_{2.5}$ concentrations of the two DustTrak DRX aerosol monitors that were used in the SMT inlet and outlet sites at various concentrations of sodium chloride (NaCl) particles. Excellent agreement was found between these two DRX. Since the DRX measures PM concentration based on light scattering, the relationship between DRX reading and PM mass changes with particle optical properties, size distribution, and density (Wang et al. 2009). Therefore, the DRX readings were further normalized to gravimetric $PM_{2.5}$ mass measured over the same sampling period and at the same site. Figure B.4 shows that the two DRXs have reasonable correlations with gravimetric $PM_{2.5}$ mass.

For VOC canister samples and continuous NO_x, CO, and CO_2 monitors used in the FMT, the measurements were not dependent on flow rate, so these methods were only checked periodically to confirm that flows were within an acceptable range. Prior to field deployment, all continuous CO, NO_x, temperature, and RH monitors were tested by operating them simultaneously in the laboratory, recording data outputs, and comparing the results for consistency. The CO and NO_x monitors were challenged with varying concentrations of target pollutant produced from zero air and certified gas standards (Scott-Marrin, Riverside, CA) by an automated gas mixer (Environics 9100), which had recently been calibrated using a reference flow standard (DryCal Definer).

Table B.4 summarizes the number of 2-hour sampling periods that were attempted for collection, excluded during QA process and remained as valid sample pairs in SMT during the 2015 study. Causes of unsuccessful collection include unexpected power outage in the power outlets where the samplers were plugged in, malfunction of timers that advance the sampling ports, pump failure, analyzer signal drift, and filter damage in the field. As will be discussed in the next section, eight NO_x sampling periods were deemed outliers due to much lower concentrations (January 21, 2015) than neighboring periods or abnormally constant readings (February 10, 2015). The first pair of $PM_{2.5}$ filters of the 2015 SMT sampling were deemed as an outlier for EF_D calculation because the outlet concentration was 22 $\mu g/m^3$ lower than the inlet concentration. Four periods of NMHC samples had concentrations near detection limit or over an order of magnitude higher than average values, indicating sampler malfunction or contamination, and were considered outliers.

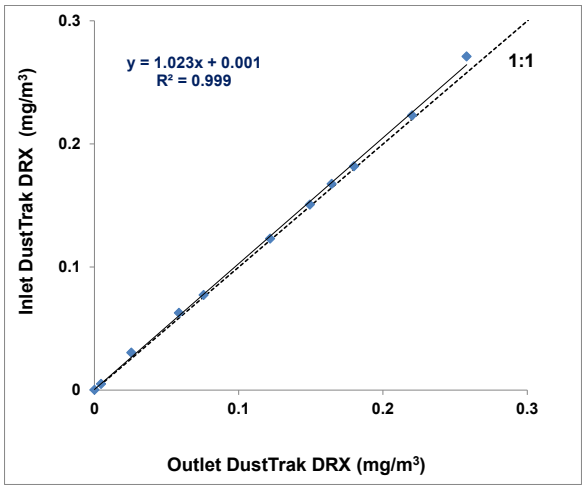

Figure B.3. Comparison of the tunnel inlet and outlet DustTrak DRX monitors using laboratory-generated sodium chloride particles before the SMT field measurement in 2015.

During the FMT field campaigns every 1-2 days the continuous monitors were challenged with known concentrations of gases (i.e., 10 ppm CO, 800 ppm CO_2, and 500 ppb NO_x) until a stable reading was obtained. The gases were introduced into the sample inlet lines directly from certified standard cylinders (Scott-Marrin or Mesa Specialty), except for NO which was blended using the Environics gas mixer and transferred in a large Tedlar bag. Baseline readings were also taken by sampling from a Tedlar bag of clean air or span gases (i.e., the NO baseline was determined during the CO span check and vice-versa). The continuous CO_2 monitors had an automatic baseline adjustment feature, so no baseline readings were needed. The periodic zero and span checks were flagged in the continuous data logs. Those logs were reviewed to determine the daily baseline and span value for each monitor and the results were tabulated, plotted as a function of time for the duration of the measurement period, and reviewed for outliers or suspect data points. A least squares linear regression equation was calculated for each monitor (separately for summer and winter campaigns). If the correlation of the baseline and span factor (i.e., $C_{actual}/(C_{indicated} - Z_{indicated})$) variation to time was statistically significant, the continuous data was adjusted using the resulting regression equation. If not statistically significant, the median value of the span factor was applied as the correction factor.

a) $PM_{2.5}$ Inlet

b) $PM_{2.5}$ Outlet

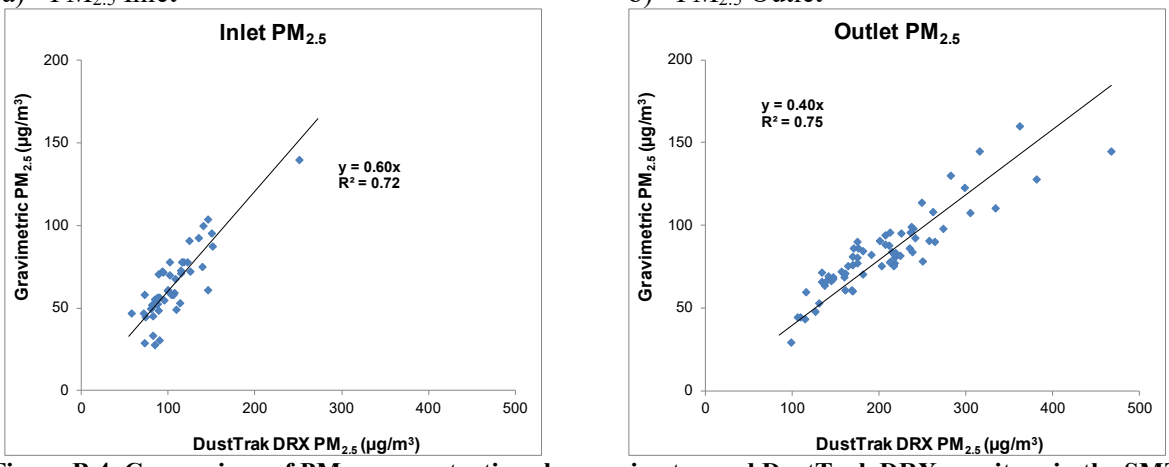

Figure B.4. Comparison of $PM_{2.5}$ concentrations by gravimetry and DustTrak DRX monitors in the SMT during the 2015 study.

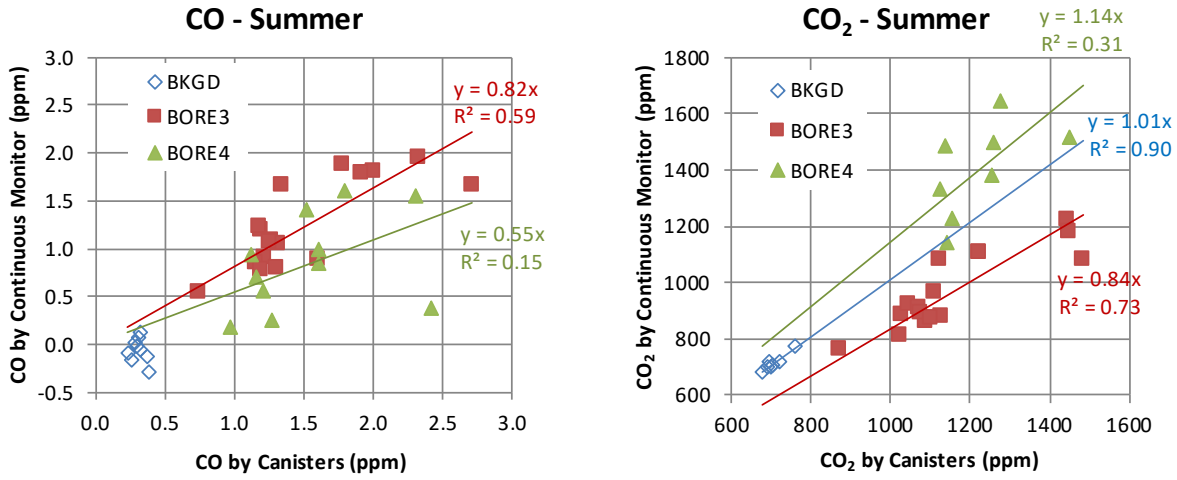

Figure B.5. Correlations between CO and CO_2 concentrations in FMT from time-averaged continuous monitors and canister analysis during the 2015 summer study.

CO and CO_2 concentrations were measured simultaneously by two methods in FMT: GC/FID analysis of canister samples and continuous non-dispersive infrared (NDIR) optical monitors. The time-averaged concentrations from the continuous monitors were compared to the corresponding canister sample results as a quality assurance check. Only the canister sample results were used in fleet-average emissions calculations. For the winter season, which did not include NDIR CO_2, the continuous CO from Bore 3 agreed well with the canister analyses yielding a high correlation (r^2 = 0.90) and +6% overall bias. The NDIR CO monitor used in Bore 4, which produced highly erratic readings due to voltage drops in the power supply, showed no significant correlation to canister data, and the data were discarded. For the summer season CO correlations for both bores were weak, probably due to high ambient temperatures adversely affecting monitor performance, but NDIR CO_2 averages correlated with canister results for all locations as shown in Figure B.5. Background CO measurements were near the detection limit for all sampling periods in both seasons.

The continuous measurement data were time-averaged to coincide with the sample collection periods and combined with results from gas and aerosol analyses. Uncertainties for the FMT time-averaged data were estimated from the variance of the calibration results as $\sqrt{(\sigma^2_{baseline} + \sigma^2_{residual})}$. The combined data for each parameter and sampling location was screened for outliers (Hubert and Vandervieren 2008). Any points identified as outliers by this method were examined and, if they were also more than 2 times larger than the next highest point and 5 times greater than the analytical uncertainty, excluded from subsequent calculations unless the discrepancy could be explained or corrected by review of the raw analytical data.

Table B.5 shows the percent of data lost at the FMT due to instrument or laboratory analysis malfunction. It also summarizes the percent of data points removed as outliers. As some of the pollutant classes have hundreds of individual compounds, we provide a range (minimum and maximum) for each pollutant class, as well as the average.

Table B.4. Summary of Attempted, Excluded, and Valid 2-Hour Sampling Periods in SMT in the 2015 Study

Species	Number of 2-Hour Sampling Periods			
	Attempted Collection	Instrument or Operator Error	Outlier	Valid Periods
CO_2	104	10	0	94
CO	104	45	0	59
NO_x	104	57	8	39
SO_2	104	16	0	88
$PM_{2.5}$	92	28	1	63
NH_3	92	27	0	65
PAHs	80	10	0	70
Carbonyls	72	13	0	59
NMHCs	72	22	4	46

Table B.5. Percentage of Data Lost at the FMT Due to Instrument or Analysis Malfunction and Removed as Outliers[a]

Pollutants	Season	Malfunction	Outliers		
			min	max	average
CO_2, CO, and CH_4	winter	0.0%	0.0%	2.2%	0.0%
	summer	0.0%	0.0%	0.0%	0.0%
NMHC	winter	0.0%	0.0%	4.3%	0.3%
	summer	0.0%	0.0%	0.0%	0.0%
NO_x	winter	8.7%	0.0%	0.0%	0.0%
	summer	4.0%	0.0%	0.0%	0.0%
Carbonyls	winter	0.0%	0.0%	4.3%	1.7%
	summer	0.0%	0.0%	2.0%	0.3%
SVOC alkanes	winter	0.0%	0.0%	1.1%	0.2%
	summer	0.0%	0.0%	0.0%	0.0%
PAH	winter	0.0%	0.0%	1.1%	0.2%
	summer	0.0%	0.0%	1.0%	0.1%
Nitro-PAH	winter	0.0%	0.0%	0.0%	0.0%
	summer	0.0%	0.0%	0.0%	0.0%
Hopanes and steranes	winter	0.0%	0.0%	0.0%	0.0%
	summer	0.0%	0.0%	1.0%	0.1%
$PM_{2.5}$, OC/EC, and elements	winter	0.0%	0.0%	0.0%	0.0%
	summer	12.0%	0.0%	0.0%	0.0%

[a] Minimum, maximum, and average numbers for outliers represent the range of data removed within each pollutant class.

After screening, the time-averaged continuous data and integrated sample analysis results were converted to consistent units ($\mu g/m^3$) with the analytes segregated by phase: gaseous, particulate, or semi-volatile (significant fraction of total mass observed on both the filter and backup adsorbent cartridge) and combined with sample information. Corresponding background (ventilation air) concentrations were then subtracted from each value measured in the two FMT bores, and the results were used as the input data for the programs used to calculate speciated emission factors for individual samples and extrapolate emissions profiles for the gasoline and diesel fueled fleets. For cases where the measured background concentration exceeded that in the tunnel, the result was set to zero ± the propagated measurement error estimate.

Evaluation of Laboratory Analyses

Laboratory data validation was conducted to ensure the internal consistency of $PM_{2.5}$ mass and chemical composition. Physical consistency was evaluated for (1) sum of measured species versus gravimetric mass; (2) reconstructed mass vs. gravimetric mass; (3) sulfate (SO_4^{2-}) versus elemental sulfur (S); (4) water-soluble potassium (K^+) versus total K; (5) calculated versus measured ammonium (NH_4^+); and (6) anion and cation balance.

The sum of $PM_{2.5}$ chemical species should be less than or equal to the corresponding gravimetric PM mass, since unmeasured species such as oxygen (O) and hydrogen (H) were not included. Figure B.6 shows a good correlation ($r = 0.91$) between sum of species and gravimetric mass, with a slope of 0.85 and an intercept of 3.78 $\mu g/m^3$. The average ratio between sum of species and gravimetric mass is 0.93±0.16, within the mass ratio limits of 0.60–1.32 set by U.S. EPA for its Chemical Speciation Network (CSN) (U.S. EPA 2012). The sum of species was greater than the gravimetric mass for 31 out of 132 measured filters. Potential causes of this overestimation are (1) sample inhomogeneity of the Teflon-membrane and quartz-fiber filters; (2) evaporation of volatile species from the Teflon-membrane filters; and (3) non-representative positive and negative carbon artifacts correction using the backup quartz-fiber filter placed behind the front quartz-fiber filter (Chow et al. 2010; 2015).

PM mass reconstruction applies a set of coefficients to measured species to estimate unmeasured components (Chow et al. 2015). The major categories are (1) organics or organic matter (OM=1.2 × organic carbon [OC] to account for unmeasured hydrogen and oxygen in fresh vehicle exhaust) (Kleeman et al. 2000); (2) elemental carbon (EC); (3) water-soluble SO_4^{2-}; (4) water-soluble nitrate (NO_3^-); (5) NH_4^+; (6) geological material (estimated as 2.2×[Al]+2.49×[Si]+1.63×[Ca]+1.94×[Ti]+2.42×[Fe]) (Malm et al. 1994); and (7) others (sum of other measured ions and elements without double counting). Figure B.6 shows that the reconstructed and measured $PM_{2.5}$ mass is correlated ($r = 0.89$) with a slope closer to unity (0.89) than that of the sum of species (0.85). The average ratio between reconstructed and gravimetric mass was 1.01±0.18, indicating valid measurements for major $PM_{2.5}$ components.
SO_4^{2-} was measured by ion chromatography (IC) using quartz-fiber filter extracts while elemental S was measured by X-ray fluorescence (XRF) on Teflon-membrane filters. Within precision estimates, the molar ratio of S to SO_4^{2-} is expected to equal to one if all sulfur exists as water-soluble SO_4^{2-} and greater than one due to the presence of water-insoluble and/or organic S. The U.S. EPA CSN limits for S to SO_4^{2-} molar ratio to be within 0.75-1.35 (U.S. EPA 2012). Figure B.6 shows that most samples were on or below the 1:1 line with a few exceptions. Possible causes of higher SO_4^{2-} than S molar concentrations are (1) volatile sulfur-containing species (e.g., H_2SO_4) were measured by IC, but were vaporized under the vacuum and higher temperature environment of the XRF analysis chamber; and (2) the filters were heavily loaded, and the X-ray may not totally penetrate the particle layer, causing underestimation of S. The IC SO_4^{2-} measurement is a more accurate measurement for both cases.

Water-soluble K^+ measured by IC on the quartz-fiber filter extracts should be equal to or less than total K measured by XRF on the Teflon-membrane filters. Figure B.6 shows a K^+/K slope of 0.58 with a low (-0.10 $\mu g/m^3$) intercept, indicating that soluble K^+ was always less than total K as expected.
NH_4^+ was directly measured by IC analysis of the quartz-fiber filter extract. To further evaluate ion measurements, calculated versus measured NH_4^+ are compared. NH_4^+ is commonly found in the chemical forms of NH_4NO_3, $(NH_4)_2SO_4$, and ammonium bisulfate (NH_4HSO_4). Ammonium chloride (NH_4Cl) concentration may be found near salt lakebeds or areas with deicing material, but their concentrations are generally low and not included in the calculation. Assuming full or partial neutralization, measured NH_4^+ can be compared with calculated NH_4^+, which is the sum of NH_4NO_3 with either $(NH_4)_2SO_4$ ($0.29 \times [NO_3^-] + 0.38 \times [SO_4^{2-}]$), or $(NH_4)HSO_4$ ($0.29 \times [NO_3^-] + 0.192 \times [HSO_4^-]$). Figure B.6 shows that the calculated and measured NH_4^+ had high correlations ($r \geq 0.98$), and the slope between calculated NH_4^+ assuming the sum of NH_4NO_3 and $(NH_4)_2SO_4$ was 1.05, indicating that NH_4^+ was fully neutralized as NH_4NO_3 and $(NH_4)_2SO_4$.

The anion and cation balance compares the sum of measured Cl^-, NO_3^-, and SO_4^{2-} to the sum of measured NH_4^+, Na^+, and K^+ in μeq/m^3, the product of mass concentration (in μg/m^3) divided by the atomic weight of the chemical species divided by the species' charge. Therefore:

$$\mu eq/m^3 \; for \; anions = \left(\frac{[Cl^-]}{35} + \frac{[NO_3^-]}{62} + \frac{[SO_4^{2-}]}{96/2} \right) \quad \text{(A1)}$$

$$\mu eq/m^3 \; for \; cations = \left(\frac{[NH_4^+]}{18} + \frac{[Na^+]}{23} + \frac{[K^+]}{39.1} \right) \quad \text{(A2)}$$

Figure B.6 shows an excellent balance between the measured anions and cations with a slope of 0.99 and r of 1.00, within the U.S. EPA CNS ion ratio limits of 0.86-2.82 (U.S. EPA 2012). The regression analysis indicates that particles were nearly neutral and adequate ions were measured.

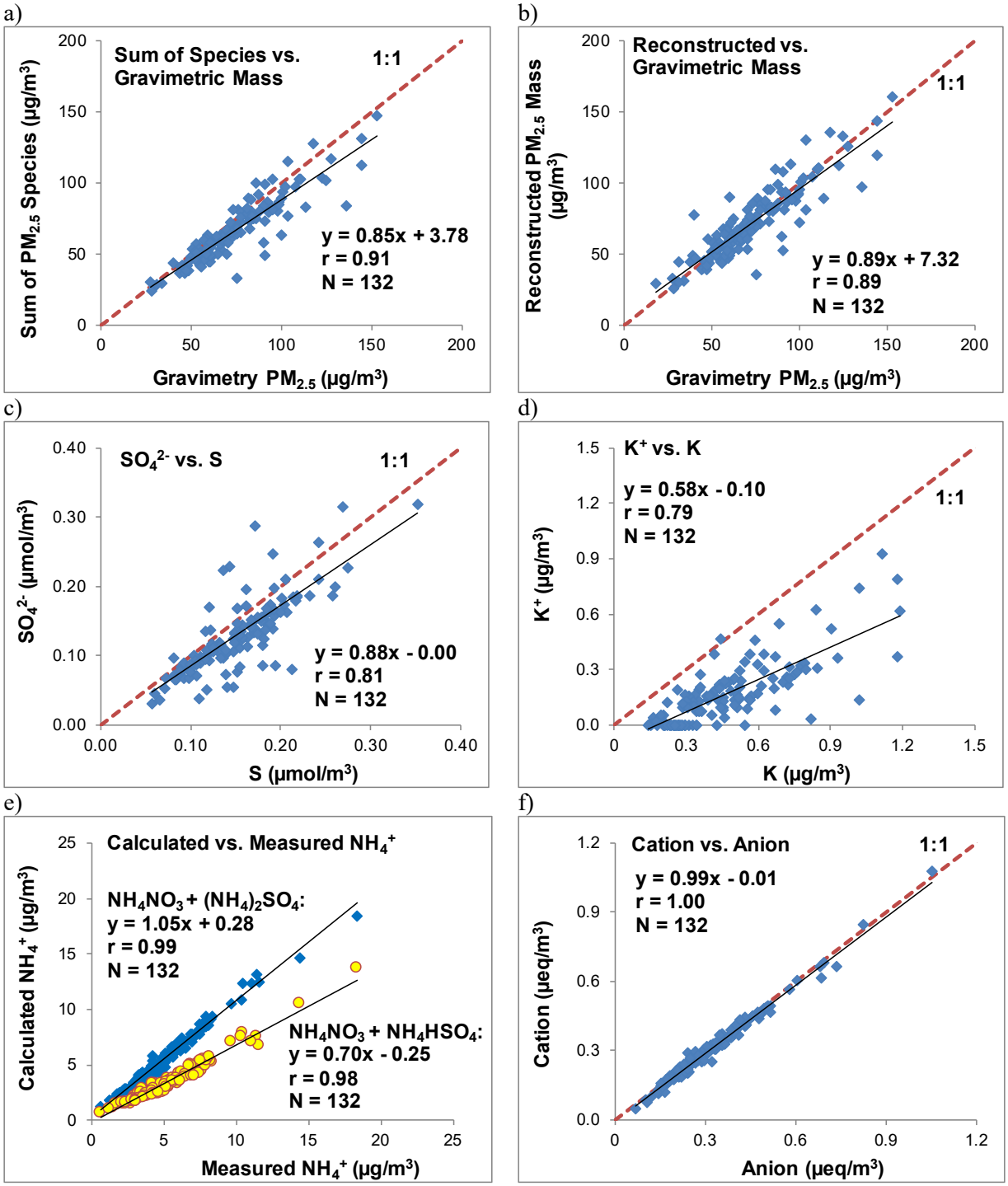

Figure B.6. Validation comparisons for SMT $PM_{2.5}$ chemical concentrations on 132 sample sets collected in the 2015 study for (a) sum of chemical species vs. gravimetric mass; (b) reconstructed vs. gravimetric $PM_{2.5}$ mass; (c) water-soluble sulfate vs. elemental sulfur; (d) water-soluble potassium ion vs. total potassium; (e) calculated vs. measured ammonium; and (f) cation vs. anion. Reconstructed mass = organics + EC + sulfate + nitrate + ammonium + geological material + others, where organics = organic carbon × 1.2, and geological material = 2.2×[Al] + 2.49×[Si] + 1.63×[Ca] + 1.94×[Ti] + 2.42×[Fe]. The calculated NH_4^+ is the sum of NH_4NO_3 with either $(NH_4)_2SO_4$ (0.29 × $[NO_3^-]$ + 0.38 × $[SO_4^{2-}]$), or $(NH_4)HSO_4$ (0.29 × $[NO_3^-]$ + 0.192 × $[HSO_4^-]$). The ion microequivalent concentrations (µeq/m^3) were the product of mass concentration (in µg/m^3) divided by the atomic weight of the chemical species and the species' charge.